Direct Numerical Simulation of 3-Dimensional Axial Turbulent Boundary Layers with Spanwise Curvature

Dong Shin Shin*
Department of Mechanical Engineering, Hong-Ik University

Direct numerical simulation has been used to study turbulent boundary layers with convex curvature. A direct numerical simulation program has been developed to solve incompressible Navier-Stokes equations in generalized coordinates with the finite volume method. We considered two boundary layer thicknesses. When the curvature effect is small, mean velocity statistics show little difference with those of a plane channel flow. Turbulent intensity decreases as curvature increases. Contours suggest that streamwise vorticities are strong where large pressure fluctuations exist.

Key Words : Direct Numerical Simulation, Axial Turbulent Boundary Layer, Spanwise Curvature

1. Introduction

Turbulent flows that evolve over surfaces with convex curvature normal to the mean flow are common in engineering applications. However, it is only for strong curvatures that the curvature effects become noticeable. For this reason, this flow has received less attention than its planar counterpart. This kind of flows occurs when sonar devices are towed by long cables. The induced noise in such flow fields can be magnified due to the high speed of the submerged vehicle and can affect the performance of the device. Therefore, the characteristics of the wall pressure fluctuations underneath the transversely curved boundary layers is of particular interest. When the boundary layer thickness is much larger than the radius, the curvature effects become strong. To achieve a large boundary layer thickness relative to the radius, experiments are typically performed over long tubes or wires. The aeroelastic interaction between the flow and the wire and the alignment of the cylinder with the mean flow are of concern. The available experimental data (Lueptow, 1988) suggest that no consesus exists on the effects of the curvature to the turbulent flow. The measurement of the wall pressure fluctuations vary among researchers (Willmarth et al., 1976). Neves *et al.* (Neves et al., 1994) studied the curvatre effects on turbulent boundary layers by direct numerical simulation with a spectral method. Choi and Moin (1990) used DNS to investigate the wall pressure fluctuations, but their Reynolds number was relatively low.

We conducted direct numerical simulation with finite volume method to overcome difficulties in the measurement of the wall pressure fluctuations and turbulent boundary layers with convex curvature. Direct numerical simulation of turbulence is an ideal tool for studying turbulent flows at low Reynolds numbers. A direct numerical simulation program has been developed to solve incompressible Navier-Stokes equations in generalized coordinates. We accumulated turbulent boundary layer data to study the effects of the curvature on the instantaneous and mean flow fields. The study also identified a parameter to separate the curvature boundary layer from its corresponding planar boundary layer.

* **E-mail** : dsshin@wow.hongik.ac.kr
TEL : +82-2-320-1477 ; **FAX** : +82-2-324-8911
Department of Mechanical Engineering, Hong-Ik University, 72-1, Sangsu-dong, Mapo-ku, Seoul 121-791, Korea. (Manuscript **Received** July 16, 1999; **Revised** January 24, 2000)

2. Numerical Method

The governing equations for an incompressible flow are

$$\frac{\partial u_i}{\partial x_i}=0 \tag{1}$$

$$\frac{\partial u_i}{\partial t}+\frac{\partial u_i u_j}{\partial x_j}=-\frac{\partial p}{\partial x_i}+\frac{1}{Re}\frac{\partial^2 u_i}{\partial x_j \partial x_j} \tag{2}$$

where x_i are the coordinates, and u_i are the corresponding velocity components. We developed the code using generalized coordinates in 1 and 2 directions and Cartesian coordinates in the 3 direction. All variables are non-dimensionalized by the boundary layer thickness δ^* and the free-stream velocity u_∞, and Re is the Reynolds number, $Re=u_\infty \delta^*/\nu$, where ν is the kinematic viscosity.

The time integration method used to solve Eqs. (1) and (2) is based on a fully implicit, fractional step method (Choi and Moin, 1990). All the spatial derivatives are approximated with the second order central difference method.

3. Axial Turbulent Boundary Layer With Spanwise Curvature

We performed direct numerical simulations of axial turbulent boundary layers with spanwise curvature. We assumed that the flow is homogeneous in the circumferential and axial directions. We considered a semi-infinite radial domain as a finite domain with $r\in[a,\ a+1]$. Here a is the nondimensionalized radius of the cylinder. The non-dimensional boundary layer thickness δ is 1. We used the boundary condition of sem-infinite domain at $r=a+1$ where the boundary layer edge is. The flow is maintained by a mild pressure gradient and the analytic laminar solutions are used as initial profiles. We used no-slip condition at the cylindrical surface.

$$\vec{u}|_{r=a}=0 \tag{3}$$

We used periodic conditions in the axial and circumferential directions. The axial nondimensional distance is L_3. In the semi-infinite radial location, the boundary conditions are $u_3 \rightarrow u_\infty$ and $u_1,\ u_2 \rightarrow 0$. We implemented the above conditions at $r=a+1$ as follows.

$$\left.\frac{\partial}{\partial r}\left(\frac{u_1}{r}\right)\right|_{r=a+1}=0$$
$$u_2|_{r=a+1}=0 \tag{4}$$
$$\left.\frac{\partial}{\partial r}\left(\frac{u_3}{r}\right)\right|_{r=a+1}=0$$

The first and third conditions mean that there are no shear stresses in the axial and circumferential directions. The second condition implies that the radial velocity should be zero at $r=a+1$ and the boundary layer does not grow in space or in time.

In order to study the effects of curvature on a axial turbulent boundary layer, we considered two bounadary layer thicknesses, $\delta/a=2$ and 5. Figure 1 shows the computational mesh used in this study.

We used a computational mesh with $64\times95\times$

Table 1 Grid resolution parameters

δ/a	2	5
L_3	4π	4π
L_3^+	2,095	2,425
$L_{\theta_i}^+=2\pi a^+$	524	243
$L_{\theta_i}^+=2\pi(a^++\delta^+)$	1,571	1,455
$\Delta_3^+=L_3^+/N_3$	10.91	12.63
$\Delta_{\theta_i}^+=L_{\theta_i}^+/N_1$	8.06	3.80
$\Delta_{\theta_o}^+=L_{\theta_o}^+/N_1$	24.17	22.73
Δr_1^+	0.028	0.032
(N_1, N_2, N_3)	(64,95,192)	(64,95,192)

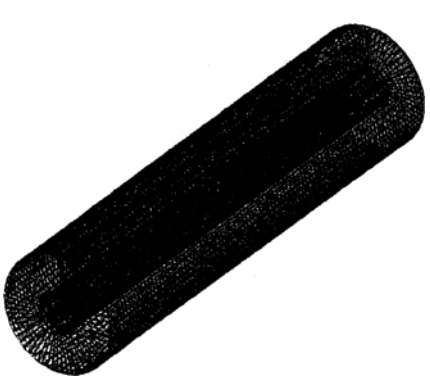

Fig. 1 Computational grids

192 nodes, and Table 1 shows the resolution of the mesh for $\delta/a=2$ and 5 cases. The meshes are uniform in the axial and circumferential directions, and the ones for the normal direction are generated from hyperbolic tangent function. As we mentioned before, the flow should have a constant mass flow rate to reach the statistically steady state, which requires a mild axial pressure gradient, $-d\bar{p}/dx_3$. The axial mass flow rate $\dot{m}$ can be written as follows.

$$\dot{m}=\int_{Ac} u_3 dA_c \tag{5}$$

To obtain the pressure gradient for a constant mass flow rate, we use the axial momentum equation.

$$\frac{\partial u_3}{\partial t}+\frac{\partial u_3 u_i}{\partial x_i}=-\frac{\partial p}{\partial x_3}+\frac{1}{Re}\nabla^2 u_3$$
$$=-\frac{d\bar{p}}{dx_3}-\frac{\partial p'}{\partial x_3}+\frac{1}{Re}\nabla^2 u_3 \tag{6}$$

Here, $d\bar{p}/dx_3$ is the pressure gradient for the constant mass flow rate and $-\partial p'/\partial x_3$ is fluctuating pressure gradient. When we integrate Eq. (6) over the whole flow field, we can get the following relation for the pressure gradient.

$$\frac{d\bar{p}}{dx_3}=-\frac{2a}{Re(2a+1)}\left.\frac{\partial u_3}{\partial r}\right|_{r=a} \tag{7}$$

Equation (7) gives the mean pressure gradient for a constant mass flow rate. The calculations have been performed until all the statistics have reached their statistically steady state. After the calculations have reached the fully developed state, all the statistics are calculated using spatial (in the circumferential and axial directions) and temporal averaging. We compared the results to those of a plane channel(Luxton et al., 1984).

Table 2 shows the mean velocity statistics for both cases as well as the plane channel ($\delta/a=0$). Since the Reynolds numbers are similar, Table 2 shows the effects of curvature in flows over transversely curved surfaces. The displacement thickness (δ^*) and momentum thickness (θ^*) for the axial turbulent boundary layer with convex curvature are obtained as follows(Lueptow et al., 1985).

$$\left(\frac{a}{\delta}+\frac{\delta^*}{\delta}\right)^2-\left(\frac{a}{\delta}\right)^2=2\int_{a/\delta}^{a/\delta+1}\left(1-\frac{\bar{u}_3}{u_\infty}\right)rdr \tag{8}$$

Table 2 Mean flow parameters

	Plane Channel	Axial Cylinder	
δ/a	0	2	5
a^+	—	83	39
C_f	6.04×10^{-3}	4.81×10^{-3}	6.46×10^{-3}
Re_δ	3,300	3,400	3,400
Re_τ	180	167	193
Re_a	—	1,700	680
δ^*/δ	0.141	0.324	0.186
θ^*/δ	0.087	0.245	0.150
H	1.62	1.33	1.24

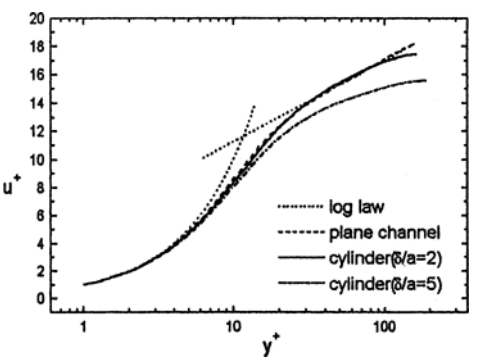

Fig. 2 Mean velocity profiles. For log law $u^+=y^+$ and $u^+=2.5\ln y^++5.5$

$$\left(\frac{a}{\delta}+\frac{\theta^*}{\delta}\right)^2-\left(\frac{a}{\delta}\right)^2=2\int_{a/\delta}^{a/\delta+1}\left(\frac{\bar{u}_3}{u_\infty}\right)\left(1-\frac{\bar{u}_3}{u_\infty}\right)rdr \tag{9}$$

Figure 2 shows the mean velocity profile of the two transversely curved flows compared to that of the plane channel flow. Because a^+'s are small, the curvature of the wall has little effect on the viscous sublayer velocity.

The mean velocity profile in the logarithmic region for $\delta/a=2$ shows a little difference from that of the plane channel. As the curvature increases ($\delta/a=5$), the slope of the mean velocity profile decreases and the profiles become convex. It shows that the mean velocity profile in the large transverse curvature case deviates from that of the plane channel flow.

Figure 3 shows the turbulence intensity normal-

ized by the friction velocity. It shows that the axial intensity is the largest and that both the normal and the azimuthal ones are almost the same. They decrease as the curvature increases. The maximum of the axial intensity moves towards the wall as the curvature increases. The decrease in turbulence kinetic energy with increasing curvature can be explained in part by the small surface area where turbulent motions are active relative to the volume of whole flow field. This result agrees well with previous experiments (Lueptow et al., 1985).

Figure 4 shows the contours of the instantaneous streamwise velocity in the plane normal to the mean flow at $z=2\pi$. It shows that $\delta/a=2$ case has 6~7 streaks around the cylinder whereas $\delta/a=5$ case has 4 streaks. A strongly curved cylinder or flows with smaller a^+ apparently supports fewer streaks.

Figures 5 and 6 show the radial velocity and streamwise vorticity on the same plane. In Figures 4~6 the regions of sweep and ejection of fluid to

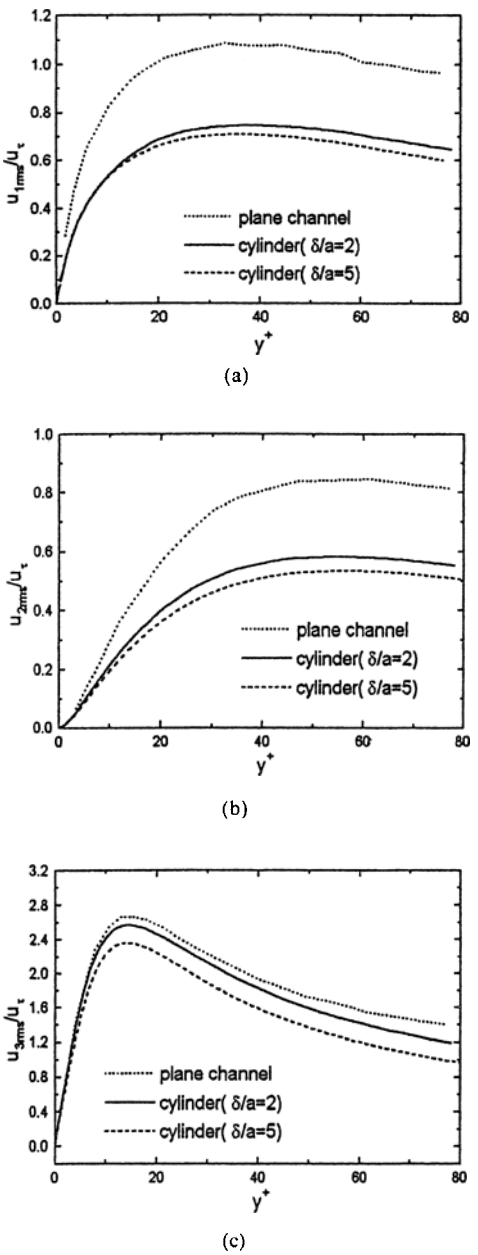

Fig. 3 Root-mean-seqare velocity fluctuations normalized by u_τ. (a) Azimuthal intensity (b) Normal intensity (c) Axial intensity

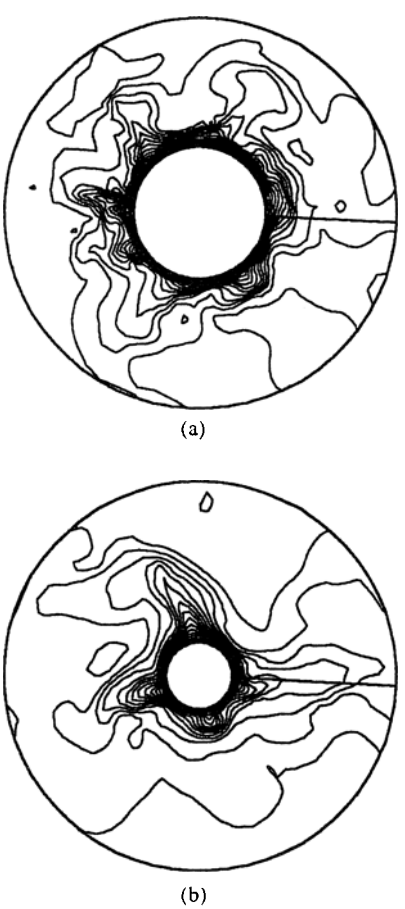

Fig. 4 Contours of normalized axial velocity (u_3/u_τ) on a plane normal to the mean velocity at $z=2\pi$. (a) $\delta/a=2$ (b) $\delta/a=5$

(a) (b)

Fig. 5 Contours of normalized radial velocity (u_2/u_τ) on a plane normal to the mean velocity at $z=2\pi$. (a) $\delta/a=2$ (b) $\delta/a=5$

(a) (b)

Fig. 6 Contours of normalized streamwise vorticity ($\omega_3\nu/u_\tau^2$) on a plane normal to the mean velocity at $z=2\pi$. (a) $\delta/a=2$ (b) $\delta/a=5$

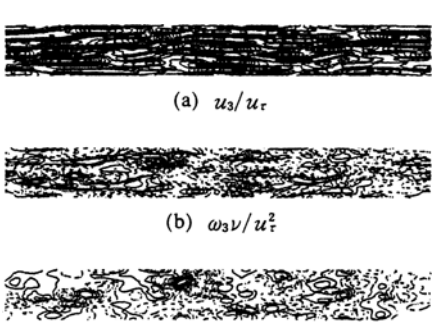

(a) u_3/u_τ

(b) $\omega_3\nu/u_\tau^2$

(c) $p/\rho u_\tau^2$

Fig. 7 Contours of normalized (a) axial velocity (b) axial vorticity and (c) pressure on an unwrapped cylindrical surface at $y^+\approx 5$. ($\delta/a=5$)

and away from the cylinder surface can be identified.

Kim et al. (1987) showed that the near-wall streamwise vortices comprise the significant source term in the pressure Poisson equation in plane channel flows. Figure 7 shows the contours of normalized streamwise velocity, vorticity, and pressure on an unwrapped cylindrical surface at $y^+\approx 5$ for $\delta/a=5$ case. Contours of streamwise velocity shows the existence of streaks near the cylinder. Figures 7(b-c) show that there are strong vorticies where significant pressure fluctuations exist. Figure 8 shows contours of normalized pressure on an unwrapped cylindrical surface. It shows little difference from the result at y^+

Fig. 8 Contours of normalized pressure on an unwrapped cylindrical surface. ($\delta/a=5$)

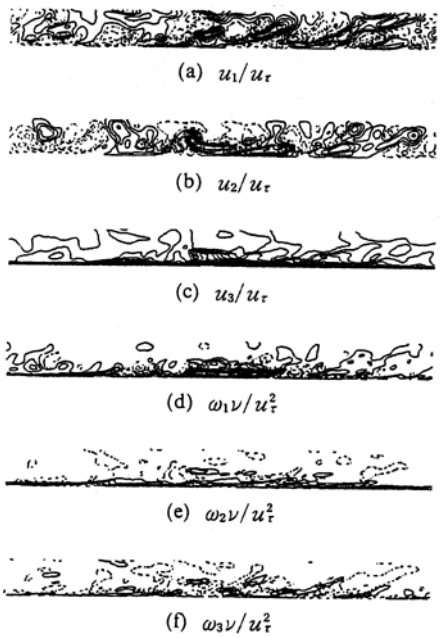

Fig. 9 Contours of velocity and vorticity at $r-z$ cross-section. ($\delta/a=5$)

≈ 5. Also in a cylindrical turbulent boundary layer, streamwise vortices seem to be an important source term for pressure fluctuations.

Figure 9 shows contours of velocity and vorticity at a $r-z$ cross-section for $\delta/a=5$ case. They show similar features to those of the plane channel but the outer layer is more quiescent than that of the plane chanel. This agrees well with the lower turbulence intensities in curved flows. Axial velocity and vorticity in Fig. 9 show streaks developing near the wall.

4. Summary

We performed a direct numerical simulation of axial turbulent boundary layers with spanwise curvature. We developed a direct numerical simulation program in generalized coordinates with finite volume method. We considered two boundary layer thicknesses-two times and five times the cylinder radius. For the small curvature case, the mean velocity statistics shows little difference from those of a plane channel flow. For the large curvature case, we observe a lower outer layer velocity than that of its planar counterpart. Turbulence intensity decreases as the curvature increases. Contours suggest that the near-wall streamwise vorticities are strong where large pressure fluctuations exist.

Acknowledgments

This work has been sponsored by Underwater Acoustics Research Center. The use of the supercomputer facilities at the Systems Engineering Research Institute is appreciated. The author would like to thank Prof. H. C. Choi at Seoul National University for his helpful advice through the work.

References

Lueptow, M. R., 1988, "Turbulent Boundary Layer on a Cylinder in Axial Flow," NUSC T. R., 8389, Naval Underwater Systems Center, New London, CT 06320.

Willmarth, W. W., R. E. Windel, L. K. Sharma and T. J. Bogar, 1976, "Axially Symmetric Turbulent Boundary Layers on Cylinders: Mean Velocity Profiles and Wall Pressure Fluctuations," *J. Fluid Mech.*, Vol. 76, pp. 35~64.

Neves, J. C., Moin, P. and Moser, R. D., 1994, "Effects of Convex Transverse Curvature on Wall -Bounded Turbulence. Part 1. The Velocity and Vorticity," *J. Fluid Mech.*, Vol. 226, pp. 349 ~381.

Choi, H. and Moin, P., 1990, "On the Space -Time Characteristics of the Wall Pressure Fluctuations," *Phys. Fluids* A, Vol. 2, pp. 1450 ~1460.

Luxton, R. E., Bull, M. K. and Rajagopalan, S., 1984, "The Thick Turbulent Boundary Layer on a Long Fine Cylinder in Axial Flow," *Aero. J.* 88, p. 186.

Lueptow, M. R., Leehey, P. and Stellinger, T., 1985, The Structure of Turbulent Boundary Layer on a Cylinder in Axial Flow. *Phys. Fluids* Vol. 28, pp. 3495~3505.

Kim, J. P., Moin, P. and Moser, R. D., 1987, "Turbulence Statistics in Fully Developed Channel Flow at Low Reynolds Number," *J. Fluid Mech.* Vol. 177, pp. 133~166.